

Effect of Shape of Sodium Salicylate Particles on Physical Property and In Vitro Aerosol Performance of Granules Prepared by Pressure Swing Granulation Method

Submitted: July 10, 2003; Accepted: October 17, 2003

Masayuki Watanabe,¹ Tetsuya Ozeki,¹ Tomoko Shibata,¹ Hayato Murakoshi,¹ Yuuki Takashima,¹ Hiroshi Yuasa,¹ and Hiroaki Okada¹

¹Department of Pharmaceutics and Drug Delivery, School of Pharmacy, Tokyo University of Pharmacy and Life Science, 1432-1 Horinouchi, Hachioji 192-0392, Japan

ABSTRACT

The purpose of this research was to investigate the effect of the shape of sodium salicylate (SS) particles on the physical properties as well as the in vitro aerosol performance of the granules granulated by the pressure swing granulation method. SS was pulverized with a jet mill (JM) to prepare the distorted particles, and SS aqueous solution was spray dried (SD) to prepare the nearly spherical particles. The particle size distribution, crushing strength, and pore size distribution of the granules were measured. The adhesive force of the primary particles in the granules was calculated according to Rumpf's equation. The in vitro aerosol performance of the granules was evaluated using a cascade impactor. Both JM and SD particles can be spherically granulated by the pressure swing granulation method without the use of a binder. The size of SD granules was smaller than that of JM granules. Although the crushing strength of the JM and SD granules is almost the same, the internal structures of JM granules and SD granules were found to differ, and the SD particles appear to have been condensed uniformly, resulting in a nearly spherical shape. In the inhalation investigation, the percentage of SS particles of appropriate size delivered to the region for treatment was noticeably higher for SD granules than for JM granules. This finding might be because the adhesive force of the SD primary particles was smaller than that of the JM primary particles in the granules and because the SD granules could be easily separated by air current to obtain the primary particles.

Corresponding Author: Tetsuya Ozeki, Department of Pharmaceutics and Drug Delivery, School of Pharmacy, Tokyo University of Pharmacy and Life Science, 1432-1 Horinouchi, Hachioji 192-0392, Japan; Tel: +81-426-76-4492; Fax: +81-426-76-4492; Email: ozekit@ps.toyaku.ac.jp

KEYWORDS: pressure swing granulation, aerosol performance, particle shape, dry powder inhalation

INTRODUCTION

Dry powder inhalation has become an attractive treatment for pulmonary and systemic diseases.¹ Dry powder inhaler (DPI) has the advantages of avoiding the use of chlorofluorocarbons as propellants and, in contrast to pressurized metered inhalation, easy synchronization with patient inspiration.²⁻¹⁰ Inhalation efficiency is influenced by the aerodynamic diameter of drug particles. The effective aerodynamic diameter range for drug particles in treatment is from approximately 0.5 μm to 7.0 μm .^{3,11,12} Particles larger than this range deposit in the oral cavity and pharynx, and particles smaller than this range are exhausted with expiration. One disadvantage of the fine particles is that they are very adhesive, thus handling them is extremely difficult.

Pressure swing granulation is a novel fluidized bed granulation method for fine cohesive powders that does not require the use of binders or other additives.^{13,14} We have applied pressure swing granulation for the first time to the granulation of pharmaceutical powders.^{15,16} In a previous study, the composite granules using 2 model powders (sodium salicylate [SS] and calcium gluconate) were granulated by the pressure swing granulation method, and the aerosol performance was studied.¹⁷ SS is an antipyretic, antiinflammatory, and antirheumatic drug, which is usually injected into a vein several times a day.¹⁸ It is possible to make a patient-friendly, pain-free formulation using dry powder inhalation. In the present study, distorted particles and almost spherical particles of SS were prepared using a jet mill (JM) and a spray drier (SD), respectively. These particles were granulated by the pressure swing granulation method, and the effect of the shape of SS particles on the physical properties as well as the in vitro aerosol performance of the granules was investigated.

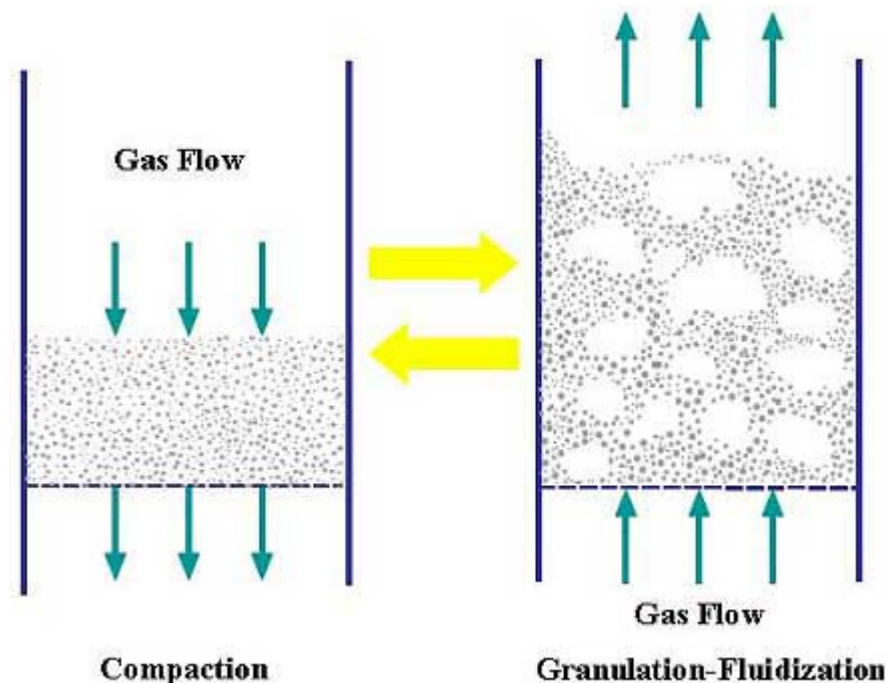


Figure 1. Principle of pressure swing granulation.

MATERIALS AND METHODS

Materials

SS (Junsei Chemical, Tokyo, Japan) was used as a model drug. The distorted particles (JM) were prepared by grinding SS with a jet mill (KIIG-1S, JM1, Dalton, Tokyo, Japan). Feed pressure and grinding pressure were 0.5 MPa. The nearly spherical particles (SD) were prepared by spraying 3% SS aqueous solution using a spray drier (Pulvis mini-spray GB22, Yamato, Tokyo, Japan) under the following conditions: feed rate, 3.5 g/min; inlet temperature, 90°C; outlet temperature, 47°C-59°C; atomizing air pressure, 3.0 kgf/cm²; and aspiration rate, 24 m³/h. JM and SD were dried *in vacuo* after preparation and stored in the desiccator.

Methods

Scanning Electron Microscope Observation

SS particles and granules were observed under a scanning electron microscope (SEM) (S-2250N, Hitachi, Tokyo, Japan). The samples were coated with gold having a thickness of 25 nm, using a quick carbon coater (SC-701C, Sanyu Electronics, Tokyo, Japan). The magnifications used were original magnification $\times 3000$ and $\times 300$.

Physical Properties of SS Particles

The density and particle size distribution of SS particles were measured using an air comparison pycnometer (model 930, Toshiba-Beckmann, Kyoto, Japan) and a particle size distribution analyzer (CAPA-700, Horiba, Kyoto, Japan). The specific surface area of SS particles was measured via the air permeability method using a powder-specific surface area measurement instrument (SS-100 type, Shimadzu, Kyoto, Japan). The time taken for air to pass through the inside of the powder bed of SS was measured and the surface area was calculated using Kozeny-Carman's equation.¹⁹ Circularity of SS particles was measured using WinROOF (Image analysis software, Mitani, Fukui, Japan) and SEM photographs. Powder x-ray diffractometer (Geigerflex RAD-IB, Rigaku, Tokyo, Japan) and differential scanning calorimeter (DSC) (DSC-8230, Rigaku) were used for studying the crystallinity of SS. The conditions were as follows for powder x-ray diffractometer: filter, Ni; voltage, 40 kV; current, 20 mA; scanning rate, 3°/min; and for DSC: heating rate, 4°C/min; N₂ gas flow, 90 mL/min.

Principle of Pressure Swing Granulation

Figure 1 shows the granulation mechanism of the pressure swing granulation method. The compaction process and the granulation-fluidization process are repeated by turns. In the compaction process, the gas flows from the upper side to the

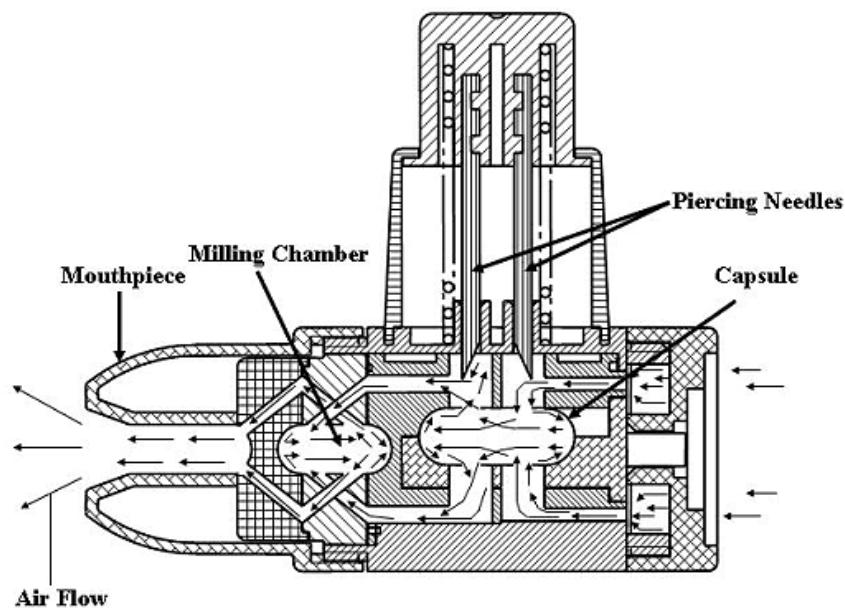


Figure 2. Structure of Jethaler reverse type inhalation device.

lower side, and the powder bed is wholly compacted. In the granulation-fluidization process, air bubbles rise through the powder bed and the powder particles are forced closed together and compacted in the particle-thick domain formed under the air bubbles. The weak areas of the aggregation are ground by a shock force and a shear stress generated by the collision between the particles and the rising of the air bubbles. Simultaneously, the aggregations become spherical because of a rotating effect. As these processes are repeated, the granules are formed mainly by the van der Waals force of the particles.¹⁴ The pressure swing granulation method enables the manufacture of granules that consist purely of drug particles.

Preparation of Granules by Pressure Swing Granulation

JM or SD were granulated into JM or SD granules using a pressure swing processor (Dalton, Tokyo, Japan) under the following conditions: loading weight, 100 g; superficial gas velocity, 425 mm/s; reservoir tank pressure, 29.4 kPa; duration of fluidization period, 15 seconds; interval between fluidization and compaction, 0.5 seconds; duration of compaction period, 1 second; and granulation time, 60 minutes.

Physical Properties of Granules

The particle size distributions of granules were measured using the image analysis method (digital microscope VH-7000, Keyence, Osaka, Japan; WinROOF image analysis software). Feret's diameter was used, and the mean particle

diameter was defined as the 50% diameter on the cumulative curve of the particle size distribution.

The crushing strength of granules of diameters ranging from 100 μm to 200 μm was measured using a microcompression testing machine (MCTE-200, Shimadzu Co, Tokyo, Japan).

The pore size distributions of granules were measured using a porosimeter (Autoscan-33, Yuasa-Ionics, Osaka, Japan), and the porosity of granules was calculated from the pore volume of granules and the density of SS.

The adhesive force between primary SS particles in the granules was calculated according to Rumpf's equation.²⁰

$$F = (\sigma \epsilon_a d_p^2) / (1 - \epsilon_a) \quad (1)$$

where F is the adhesive force (N), σ is the crushing strength of granules (Pa), ϵ_a is the porosity of granules, and d_p is the primary particle diameter.

Evaluation of In Vitro Aerosol Performance

In vitro aerosol performance of SS from SS powder or SS granules was evaluated using a cascade impactor (Andersen nonviable sampler, AN-200, Tokyo dyrec, Tokyo, Japan). A Jethaler reverse type inhalation device (Hitachi Unisia Automotive, Kanagawa, Japan) was used as the inhalation device (**Figure 2**).^{21,22} This inhalation device was equipped with a milling chamber, in which the aggregate of drug is ground into fine particles in the air stream inhaled as shown in **Figure 2**. Twenty milligrams of SS powder or SS granules^{6,17,21-23} was filled into hydroxypropyl methylcellulose

Table 1. Physical Properties of Drug Particles*

	Density (g/cm ³) [†]	Particle Size (μm) [‡]	Specific Surface Area (cm ² /g) [§]	Circularity
JM	1.53	3.09	27 100	0.573
SD	1.49	2.41	15 000	0.767

*JM indicates distorted particles; SD, nearly spherical particles.

[†]Density was measured with an air comparison pycnometer.

[‡]Particle size was measured with a particle size distribution analyzer.

[§]Specific surface area was measured by the air permeability method.

^{||} $C = 4\pi \times S_p / (l_c)^2$, where C is circularity ($0 < C \leq 1$);

S_p is projected area; and l_c is the length of circumference.

capsule (size No. 2) (Shionogi Qualicaps, Nara, Japan). The inhalation test was performed at an inhalation rate of 28.3 L/min for 5 seconds. The calibration of the flow rate was performed several times using the inhaler with an empty capsule, and then the inhalation study was performed. The quantity of the SS was assayed using a spectrophotometer (U-best 30, JASCO, Tokyo, Japan) at 295 nm. The particles in the range of aerodynamic diameter that is effective for treatment are approximately 0.5-7 μm.^{3,11,12}

The stages where these particles deposit corresponded to 2, 3, 4, 5, 6, and 7 stages of the cascade impactor (0.4-6.8 μm). The fine particle fraction (FPF), which is the total percentage deposition at stages 2 to 7 of the cascade impactor, was used to evaluate the aerosol performance. A higher FPF deposition percentage is thought to be an indicator of higher in vitro aerosol performance.

RESULTS AND DISCUSSION

Physical Properties of Primary SS Particles

Figure 3 and Table 1 show SEM photographs and the physical properties of the JM and SD primary particles, respectively. The shape of JM was distorted, but the SD had a higher circularity than did the JM. The densities of JM and SD were similar. The specific surface area of JM was large, almost twice that of SD, because of the distorted shape of JM. Figure 4 shows the particle size distribution of the primary particles of JM and SD. The particle size distributions were sharp in both JM and SD and they were fine particles under 6 μm. The mean particle diameters (D_{50}) of the JM and SD particles were approximately 3.09 and 2.41 μm, respectively (shown in Table 1). The powder x-ray diffractometry and DSC suggested that SD was almost amorphous and that the crystallinity of JM was decreased compared with that of original SS but not completely amorphous.

Physical Properties of SS Granules

Figure 5 shows SEM photographs of JM and SD granules granulated with JM and SD, respectively. Both JM and SD

particles can be spherically granulated by pressure swing granulation without the use of a binder. Figure 6 shows the particle size distribution of the granules. The size of SD granules was smaller than that of JM granules, and the mean particle diameters (D_{50}) of the JM and SD granules were approximately 230 and 160 μm, respectively.

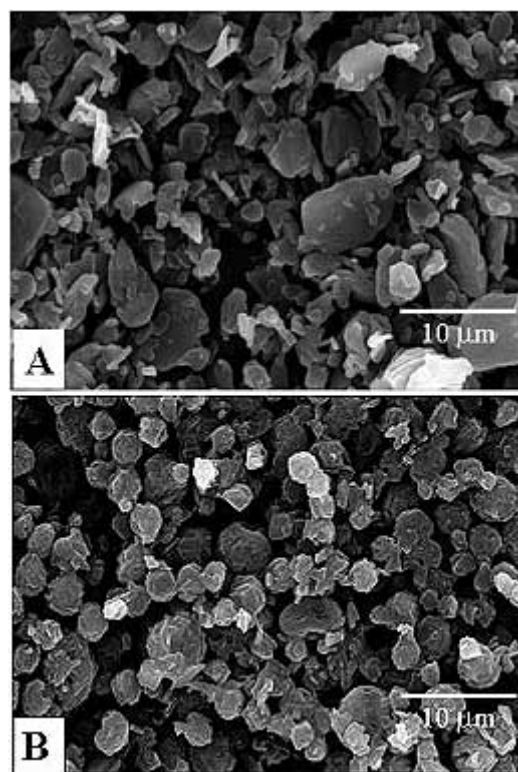


Figure 3. SEM photographs of SS particles (A) JM and (B) SD. (Original magnification is $\times 3$).

Figure 7 shows the pore size distribution of the JM or SD granules. The porosities of JM and SD were approximately equal at 0.53 and 0.51, respectively. However, the internal structures of JM granules and SD granules were found to differ. The pore size distribution of the SD granules showed a sharp peak at approximately 0.6 μm, whereas the pore size distribution of the JM granules showed 2 broad peaks at approximately 1.0 μm and 0.4 μm. The SD particles appear

to have been condensed uniformly, resulting in a nearly spherical shape. In contrast, the shape of JM particles was distorted, forming a flake-like shape, thus making uniform condensation of the JM particles difficult. The crushing strengths of the JM and SD granules were approximately 30 and 25 kPa, respectively. The adhesive forces between primary particles of JM and SD calculated using Rumpf's equation were 3.2 and 1.5×10^{-7} N, respectively.

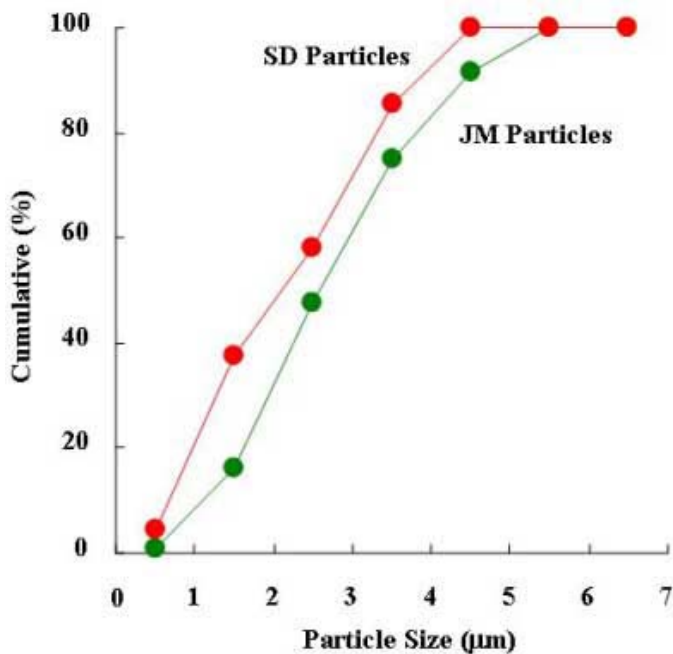


Figure 4. Particle size distribution of JM and SD primary particles.

Although the SD particles appear to have been condensed uniformly, the adhesive force of the SD primary particles is smaller than that of the JM. Since the shape of the JM particles is distorted, and the specific surface area effective for adhesion is larger than that of the SD particles, as shown in **Figure 3** and **Table 1**, the JM particles may have adhered to each other not only by point contact but also by surface contact with other JM particles. Conversely, the spherical SD particles are thought to have adhered to each other by mainly point contact. These different contact behaviors and surface areas of the primary particles may cause the adhesive force in the SD granules to be smaller than in the JM granules. In the size distribution of the JM and SD granules, shown in **Figure 6**, the D_{50} of the SD granules was smaller than that of the JM granules. SD could not grow larger granules because of the smaller adhesive force of the SD primary particles as compared with the JM primary particles.

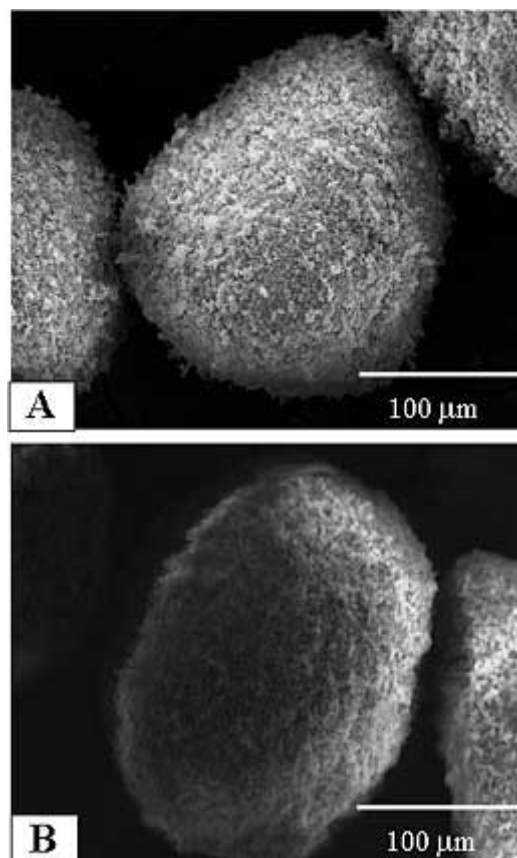


Figure 5. SEM photographs of (A) JM granules and (B) SD granules. (Original magnification is $\times 300$).

Evaluation of In Vitro Aerosol Performance

Figure 8 shows the in vitro aerosol performance of the JM and SD powders. In both cases, the residual percentage in a capsule was very high and deposition percentage in FPF was low. The deposition percentage of FPF from the SD powder was slightly higher than that from the JM powder.

Figure 9 shows the in vitro aerosol performance of the JM and SD granules prepared by pressure swing granulation of JM and SD powders, respectively. For both JM and SD granules, the residual percentage in a capsule decreased noticeably and the deposition percentage in FPF increased markedly compared with the powders shown in **Figure 8**. In the granule system, most of the JM and SD granules were emitted from the capsule, but the JM showed a high residual percentage in the device and a low deposition percentage of FPF. In contrast, the SD showed a very high deposition percentage of FPF (approximately 40%). There are reports concerning Easyhaler, Turbuhaler, and TAIFUN with high FPF (about 20% to 50%) in the inhaler commercially available.²⁴⁻²⁸ Considering that our granules contain neither binder nor carrier, 40% of FPF may be of sufficient value.

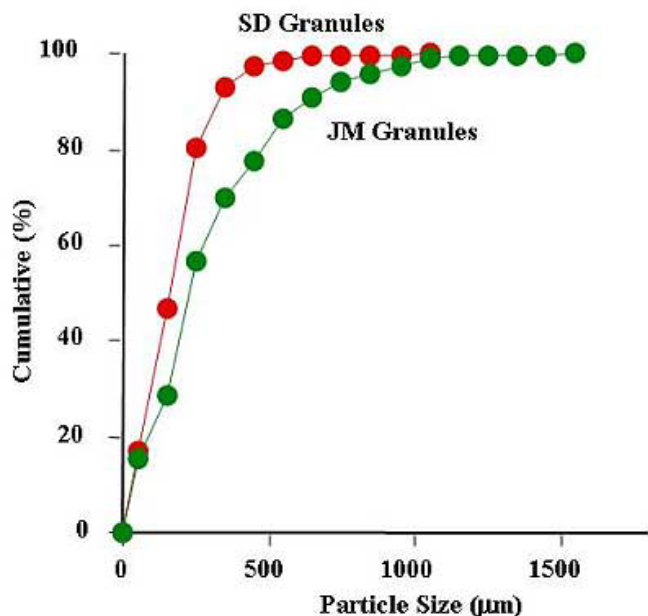


Figure 6. Particle size distribution of JM and SD granules.

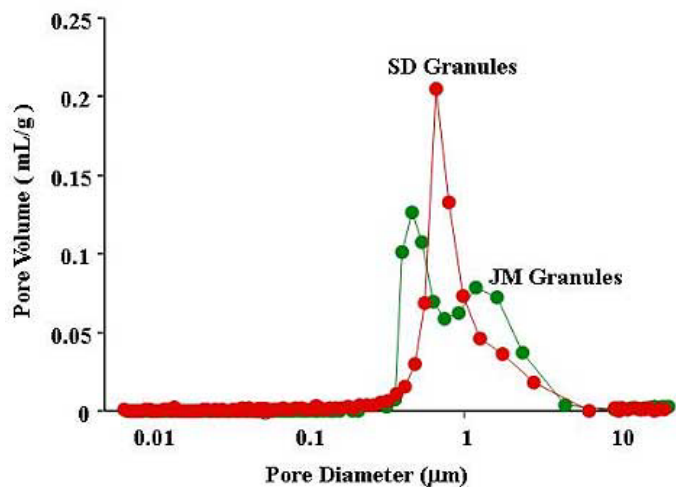


Figure 7. Pore size distribution of granules of JM and SD granules.

Effect of Adhesive Force Between Primary SS Particles on In Vitro Aerosol Performance

Figure 10 shows the relationship between the adhesive force and the deposition percentage of FPF. The SD granules, having a smaller adhesive force between primary particles, showed a higher deposition percentage of FPF. As mentioned above, the JM particles may have adhered to each other not only by point contact but also by surface contact with other JM granules; however, the spherical SD par

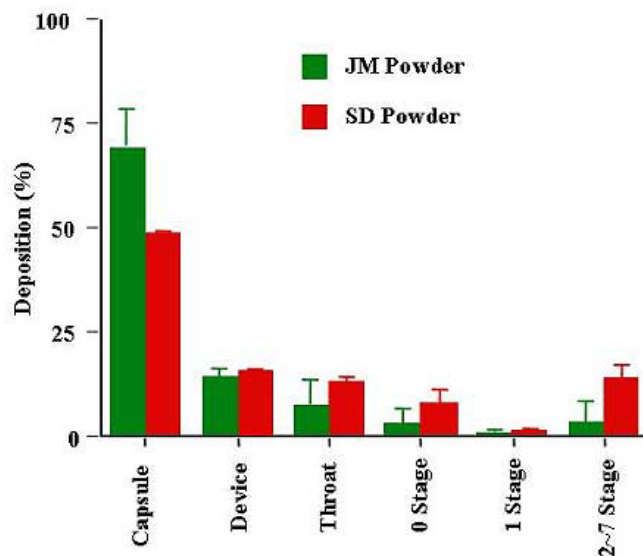


Figure 8. Comparison of aerosol performance of JM and SD powders. Each point represents the mean \pm SD (n = 3).

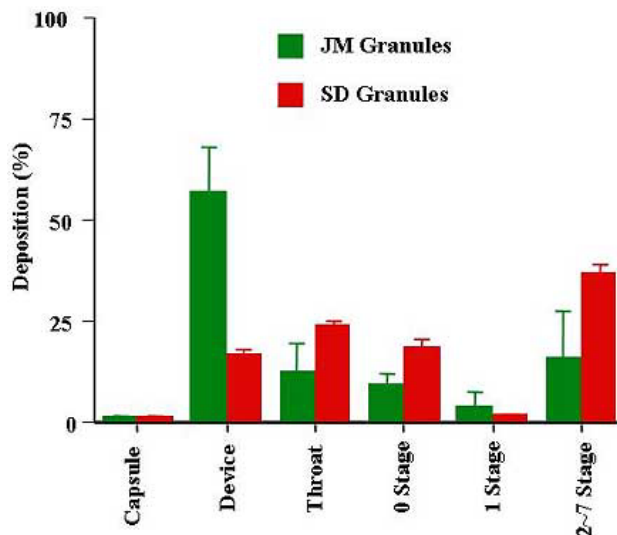


Figure 9. Comparison of aerosol performance of JM and SD granules. Each point represents the mean \pm SD (n = 3).

ticles are thought to have adhered to each other by mainly point contact. These different contact behaviors may cause the adhesive force in the SD granules to be smaller than in the JM granules. Therefore, compared with the JM granules, the SD granules were easily separated by air current to obtain the primary particles, resulting in a higher deposition percentage of FPF.

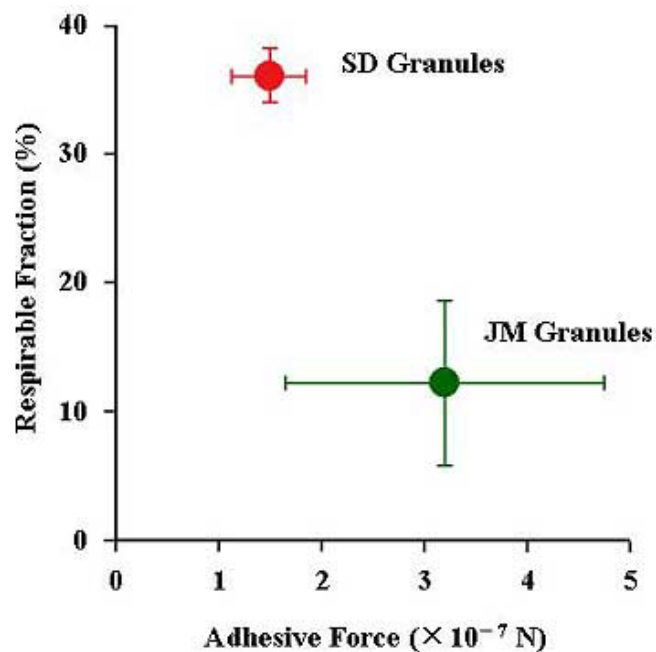


Figure 10. Effect of aerosol performance on adhesive force. Each point represents the mean \pm SD (respirable fraction, n = 3; adhesive force, n = 20).

CONCLUSION

Both JM and SD particles can be spherically granulated by the pressure swing granulation without the use of binder. The SD granules showed a higher percentage of FPF deposition, approximately 40%, compared with the JM granules. In the present study, granules consisting of nearly spherical primary SS particles prepared by pressure swing granulation were found to have a much greater DPI than DPI using ground particles.

REFERENCES

1. Timsina MP, Martin GP, Marriott C, Ganderton D, Yianneskis M. Drug delivery to the respiratory tract using dry powder inhalers. *Int J Pharm.* 1994;101:1-13.
2. Geldart D. Types of gas fluidization. *Powder Technol.* 1973;7:285-292.
3. Newman SP, Hollingworth A, Clark AR. Effect of different modes of inhalation on drug delivery from a dry powder inhaler. *Int J Pharm.* 1994;102:127-132.
4. Clark, AR. Medical aerosol inhalers: past, present, and future. *Aerosol Sci Technol.* 1995;22:374-391.
5. Steckel H, Muler B. In vitro evaluation of dry powder inhalers: influence of carrier particle size and concentration on in vitro deposition. *Int J Pharm.* 1997;154:31-37.
6. Hino T, Serigano T, Yamamoto H, Takeuchi H, Niwa T, Kawashima Y. Particle design of Wogon extract dry powder inhalation aerosols with granulation method. *Int J Pharm.* 1998;168:59-68.

7. Kawashima Y, Serigano T, Hino T, Yamamoto H, Takeuchi H. Effect of surface morphology of carrier lactose on dry powder inhalation property of pranlukast hydrate. *Int J Pharm.* 1998;172:179-188.
8. Keller M. Innovations and perspectives of metered dose inhalers in pulmonary drug delivery. *Int J Pharm.* 1999;186:81-90.
9. Karhu M, Kuikka J, Kauppinen T, Bergstrom K, Vidgren M. Pulmonary deposition of lactose carriers used in inhalation powders. *Int J Pharm.* 2000;196:95-103.
10. Staniforth JN, Rees JE. Electrostatic charge interactions in ordered powder mixes. *J Pharm Pharmacol.* 1982;34:69-76.
11. Davies PJ, Hanlon GW, Molyneux AJ. An investigation into the deposition of inhalation aerosol particles as a function of air flow rate in a modified "Kirk lung." *J Pharm Pharmacol.* 1976;28:908-911.
12. Vidgren M, Karkkainen A, Karjalainen P, Paronen P, Nuutinen J. Effect of powder inhaler design on drug deposition in the respiratory tract. *Int J Pharm.* 1988;42:211-216.
13. Nishii K, Ito Y, Kawashima N, Horio M. Pressure swing granulation, a novel binderless granulation by cyclic fluidization and gas flow compaction. *Powder Technol.* 1996;74:1-6.
14. Mikami T, Kamiya H, Horio M. Numerical simulation of cohesive powder behavior in fluidized bed. *Chem Eng Sci.* 1988;53:1927-1940.
15. Yuasa H, Higashi S, Ozeki T. Preparation of granules for dry powder inhaler by pressure swing granulation method and drug particle delivery. *J Pharm Sci Technol Jpn.* 2002;62:67-79.
16. Yuasa H, Higashi S, Ozeki T. Granulation for dry powder inhaler granules having low hardness by pressure swing granulation method and drug particle delivery in using several kinds of inhalation devices. *J Japan Soc Pharm Machinery Eng.* 2002;11:6-12.
17. Watanabe M, Ozeki T, Torii Y, Shibata T, Murakoshi H, Takashima Y, Yuasa H, Okada H. Preparation of two-drug composite granules for dry powder inhalation by pressure swing granulation method and evaluation of their in vitro aerosol performance to lung. *J Pharm Sci Technol Jpn.* 2003;63:148-157.
18. The Handbook of the Japanese Pharmacopoeia. 14th ed. Tokyo, Japan: Hirokawa Publishing Co; 2001:C1383-C1386.
19. The Handbook of the Japanese Pharmacopoeia. 14th ed. Tokyo, Japan: Hirokawa Publishing Co; 2001:B569-B576.
20. Rumpf H. Zur theorie der zugfestigkeit von agglomeraten bei kraftubertragung an kontaktpunkten. *Chem Ing Tech.* 1970;42:538-540.
21. Ikegami K, Kawashima Y, Takeuchi H, Yamamoto H, Mimura K, Momose D, Ouchi K. A new spherically agglomerated drug composite system with lactose for dry powder inhalation. *Adv Powder Technol.* 2003;14:215-229.
22. Ikegami K, Kawashima Y, Takeuchi H, Yamamoto H, Mimura K, Momose D, Ouchi K. A new agglomerated KSR-592 b-form crystal system for dry powder inhalation formulation to improve inhalation performance in vitro and in vivo. *J Control Release.* 2003;88:23-33.
23. Hino T, Serigano T, Yamamoto H, Takeuchi H, Niwa T, Kawashima Y. Assessment of inertial separation techniques used for pressurized metered dose inhalers to evaluate respiratory deposition of aerosolized Wogon extract dry powder in vitro. *STP Pharmacia Sciences.* 1997;7:307-314.
24. Pitcairn GR, Lankinen T, Seppala OP, Newman SP. Pulmonary drug delivery from the Taifun dry powder inhaler is relatively independent of the patient's inspiratory effort. *J Aerosol Med.* 2000;13:97-104.
25. Newman SP, Pitcairn GR, Adkin DA, Vidgren MT, Silvasti M. Comparison of beclomethasone dipropionate delivery by easyhaler dry powder inhaler and pMDI plus large volume spacer. *J Aerosol Med.* 2001;14(2):217-225.

26. Hirst PH, Bacon RE, Pitcairn GR, Silvasti M, Newman SP. A comparison of the lung deposition of budesonide from Easyhaler, Turbuhaler and pMDI plus spacer in asthmatic patients. *Respir Med.* 2001;95:720-727.
27. Harjunen P, Lehto VP, Martimo K, Suihko E, Lankinen T, Paronen P, Jarvinen K. Lactose modification enhance its drug performance in the novel multiple dose Taifun DPI. *Eur J Pharm Sci.* 2002;16:313-321.
28. Kinnarinen T, Jarho P, Jarvinen K, Jarvinen T. Pulmonary deposition of a budesonide/gamma-cyclodextrin complex in vitro. *J Control Release.* 2003;90:197-205.